This is the accepted manuscript made available via CHORUS. The article has been published as:

# Characterizing random-singlet state in two-dimensional frustrated quantum magnets and implications for the double perovskite math xmlns="http://www.w3.org/1998/Math/MathML">msub>mrow>mi>Sr/mi>/mrow>mn>2/mn>/msub>msub>mrow>mi>CuTe/mi>/mrow>mrow>mn>1/mn>mo>−/mo>mi>x/mi>/mrow>/msub>msub>mrow>mi mathvariant="normal">W/mi>/mrow>mi>x/mi>/msub>msub>mrow>mi mathvariant="normal">O/mi>/mrow>mn>6/mn>/msub>/math>

Huan-Da Ren, Tian-Yu Xiong, Han-Qing Wu, D. N. Sheng, and Shou-Shu Gong

Phys. Rev. B **107**, L020407 — Published 19 January 2023

DOI: 10.1103/PhysRevB.107.L020407

# Characterizing Random-singlet State in Two-dimensional Frustrated Quantum Magnets and Implications for the Double Perovskite $Sr_2CuTe_{1-x}W_xO_6$

Huan-Da Ren[1,2], Tian-Yu Xiong[1], Han-Qing Wu[3],* D. N. Sheng[4],† and Shou-Shu Gong[1]‡
[1]*Department of Physics, Beihang University, Beijing, 100191, China*
[2]*Department of Physics, Tsinghua University, Beijing, 100084, China*
[3]*School of Physics, Sun Yat-Sen University, Guangzhou, 510275, China*
[4]*Department of Physics and Astronomy, California State University Northridge, Northridge, California 91330, USA*

Motivated by experimental observation of the non-magnetic phase in the compounds with frustration and disorder, we study the ground state of the spin-$1/2$ square-lattice Heisenberg model with randomly distributed nearest-neighbor $J_1$ and next-nearest-neighbor $J_2$ couplings. By using the density matrix renormalization group (DMRG) calculation on cylinder system with circumference up to 10 lattice sites, we identify a disordered phase between the Néel and stripe magnetic phase with growing $J_2/J_1$ in the presence of strong bond randomness. The vanished spin-freezing parameter indicates the absence of spin glass order. The large-scale DMRG results unveil the size-scaling behaviors of the spin-freezing parameter, the power-law decay of the average spin correlation, and the exponential decay of the typical spin correlation, which all agree with the corresponding behavior in the one-dimensional random singlet (RS) state and characterize the RS nature of this disordered phase. The DMRG simulation also provides new insight and opportunities for characterizing a class of non-magnetic states in two-dimensional frustrated magnets with disorder. We also compare with existing experiments and suggest more measurements for understanding the spin-liquid-like behaviors in the double perovskite $Sr_2CuTe_{1-x}W_xO_6$.

*Introduction.* Spin liquid (SL) is an exotic quantum liquid state realized in frustrated magnets[1–5], which exhibits long-range entanglement and fractionalized excitations[6–8] and may have potential applications in quantum computation[9]. After extensive search for decades, spin-liquid-like behaviors have been reported in frustrated antiferromagnets[3–5]. In particular, most of the SL candidates have been characterized as gapless spin-liquid states in experiment[4,10–16]. Nevertheless, theoretical studies have only established SL states in few highly frustrated models including kagome antiferromagnet and triangular-lattice Heisenberg models with competing interactions[3,5]. Only considering frustrated interactions may be insufficient to account for the widely observed spin-liquid-like behaviors in materials.

Another common factor that may suppress magnetic order is disorder, which naturally exists in materials[11,12,17,18]. In one dimension (1d), the strong-disorder renormalization group has established the infinite-randomness fixed point (IRFP) with infinite dynamic exponent, which describes the random singlet (RS) state in random spin chains[19–27]. A characteristic feature of the 1d RS state is the drastic difference between the average and the typical spin correlations, which follow the $r^{-2}$ power-law and the exponential decay respectively as a function of distance $r$ due to the logarithmically broad probability distribution of spin correlation[23]. By extensive experimental studies on random spin chain compounds[28–34], recently the RS behaviors have been reported in the compounds $BaCu_2(Si_{1-x}Ge_x)_2O_7$ and $Ba_5CuIr_3O_{12}$[33,34]. In two dimensions (2d), it has been shown in experiment that increased disorder can also melt magnetic order and induce spin-liquid-like behaviors[35–39]. However, understanding disorder effect in 2d frustrated systems is a longstanding challenge for theoretical study. Although the IRFP has been found in few 2d systems[40–43], the disorder-induced states in general frustrated Heisenberg models are quite elusive[44–46]. Recently, systematic exact diagonalization (ED) studies have unveiled a disordered phase driven by random couplings in various frustrated Heisenberg models, which is conjectured to be a 2d RS state[47–53]. The ED results of the dynamical and thermodynamic properties of this state qualitatively agree with the predictions of gapless spin liquids[47–54]. Nonetheless, the characteristic properties of the RS state such as the scaling behaviors of spin correlations have not been addressed and it is unresolved whether this disordered phase is indeed a RS state or not. A recent quantum Monte Carlo (QMC) study on the random $J-Q$ model find a disordered state with the average spin correlation decaying algebraically as $r^{-2}$, which is proposed as the 2d analog of the RS state although the dynamic exponent is finite[55]. It is also conjectured that such a state should also exist in the frustrated 2d Heisenberg spin systems with randomness[55], which however has not been identified. Therefore, understanding the spin correlation behaviors is highly desired to identify the nature of the disorder-induced exotic state in 2d frustrated systems.

In this Letter, we use the large-scale density matrix renormalization group (DMRG) calculation to address the characteristic behaviors of spin correlations in the disorder-induced phase. We study the spin-$1/2$ square-lattice Heisenberg model with the random nearest-neighbor (NN) $J_1$ and next-nearest-neighbor (NNN) $J_2$ couplings. This system may be considered as the preliminary description of the spin-liquid-like phase in the double perovskite $Sr_2CuTe_{1-x}W_xO_6$[56–64], which realizes simultaneous tuning of frustration and disorder by the random Te-W cation mixing. The pure $J_1-J_2$ square Heisenberg model has a non-magnetic phase near $J_2/J_1=0.5$ due to strong frustration[65–68]. With random couplings, recent ED study has found evidence for a disordered phase and a possible spin glass phase[52], without resolving the nature of the disordered phase. Based on the DMRG results, we identify a disordered phase without any magnetic order or spin glass order[44] in the strong randomness regime. Furthermore, we unveil the $L_x^{-1/2}$ scaling of the spin-freezing parameter with sys-

tem length $L_x$, the $r^{-2}$ power-law decay of the average spin correlation, and the exponential decay of the typical spin correlation, which all agree with the corresponding behavior in the 1d RS state[23] and characterize the RS nature of this disordered state. The consistent $r^{-2}$ behavior of average spin correlation also indicates that this state may belong to the same fixed point as the proposed RS state in the $J-Q$ model, which demonstrates the robust universal behavior for such interacting and disorder systems. The vanished spin-freezing parameter in our model study implies that the spin glass order should be absent in $Sr_2CuTe_{1-x}W_xO_6$ at low temperature. Our results agree with the observations in the $\mu$SR measurements of $Sr_2CuTe_{1-x}W_xO_6$, including the absent spin freezing for $x = 0.5$ at very low temperature[56] and the large dynamic exponent supporting the intermediate RS phase[64].

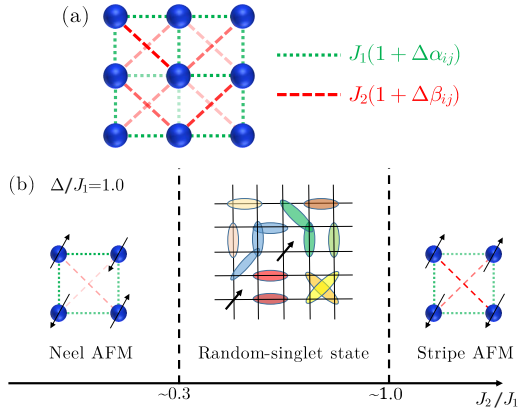



FIG. 1. Model Hamiltonian and quantum phase diagram of spin-1/2 $J_1-J_2$ square-lattice Heisenberg model with random couplings. (a) The random NN $J_1$ (green bonds) and NNN $J_2$ (red bonds) couplings are uniformly distributed in the interval $\alpha_{ij}, \beta_{ij} \in [-1, 1]$. $\Delta$ is the strength of the randomness. (b) Quantum phase diagram of the model with growing $J_2/J_1$ and fixed $\Delta/J_1 = 1$, which shows a random-singlet phase between the Néel and stripe magnetic phase.

The model with random $J_1, J_2$ couplings is defined as

$$H = \sum_{\langle ij\rangle} J_1(1+\Delta\alpha_{ij})\mathbf{S}_i\cdot\mathbf{S}_j + \sum_{\langle\langle ij\rangle\rangle} J_2(1+\Delta\beta_{ij})\mathbf{S}_i\cdot\mathbf{S}_j, \quad (1)$$

where $\alpha_{ij}$ and $\beta_{ij}$ denote the random variables uniformly distributing in the interval $[-1, 1]$, and $\Delta$ controls the randomness strength of the interval $[J_i(1-\Delta), J_i(1+\Delta)]$ $(i = 1, 2)$. We set $J_1 = 1.0$ and choose $\Delta/J_1 = 1.0$ to focus on the strong randomness case. By using the DMRG with spin SU(2) symmetry[69,70], we simulate the system on the cylinder geometry with the periodic boundary conditions along the circumference direction ($y$) and the open boundary conditions along the axis direction ($x$), with $L_y$ and $L_x$ being the numbers of sites along the two directions. We study the systems with $L_y$ up to 10. To avoid edge effects, we choose $L_x = 2L_y$ in most calculations and compute physical quantities using the middle $L_y \times L_y$ subsystem, which is found valid by the agreement of our data with the QMC result. We keep 3000 SU(2) states (equivalent to about 12000 U(1) states) to ensure the truncation error smaller than $1 \times 10^{-5}$. We take 100 (50) random samples for $L_y = 4, 6$ ($L_y = 8, 10$), which ensure the good sample average of the quantities; see Supplemental Materials (SM)[71]. We use "$\langle\rangle$" and "[ ]" to represent quantum mechanical and stochastic averages, respectively.

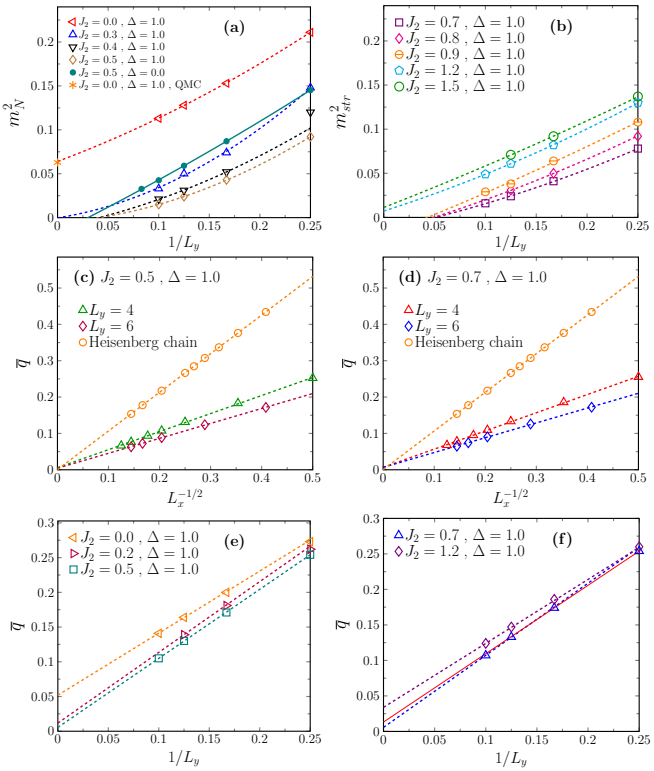



FIG. 2. Finite-size scaling of order parameters. (a) and (b) are the Néel ($m_{\rm N}^2$) and stripe ($m_{\rm str}^2$) order parameters versus $1/L_y$. For a comparison, we include the result of $J_2 = 0.5, \Delta = 0$[67], which has been identified as a non-magnetic state. The lines denote the polynomial fitting of the data up to the second order of $1/L_y$. The star symbol denotes the QMC result[72]. (c) and (d) are the spin-freezing parameter $\overline{q}$ versus $L_x^{-1/2}$ with $L_y = 4, 6$. The result of the 1d RS state of the Heisenberg chain is also shown. The good linear fittings indicate $\overline{q} \propto L_x^{-1/2}$. (e) and (f) are the spin-freezing parameter $\overline{q}$ versus $1/L_y$ obtained in the middle $L_y \times L_y$ subsystem. The dashed lines denote the linear fitting using the two largest-size data. The solid line in (f) shows the linear scaling of the small-size data with $L_y = 4$ and 6.

*Phase diagram and absent spin glass order.* We first determine the phase diagram of the system by computing magnetic order and spin-freezing parameters. We define magnetic order parameter at the wave vector $\mathbf{k}$ as

$$m^2(\mathbf{k}) = \frac{1}{N_s^2}\sum_{i,j}[\langle\mathbf{S}_i\cdot\mathbf{S}_j\rangle]e^{i\mathbf{k}\cdot(\mathbf{r}_i-\mathbf{r}_j)}, \quad (2)$$

where $N_s = L_y \times L_y$. The Néel and stripe magnetic order parameters can be defined as $m_{\rm N}^2 = m^2(\pi, \pi)$ and $m_{\rm str}^2 = (m^2(0, \pi) + m^2(\pi, 0))/2$, where the results at $(0, \pi)$ and $(\pi, 0)$ are averaged to reduce geometry effect. In Fig. 2(a-b), we show the polynomial size scaling of $m_{\rm N}^2$ and $m_{\rm str}^2$. For $J_2 = 0$, $m_{\rm N}^2$ is smoothly extrapolated to 0.064 in the $N \to \infty$

limit, which agrees with the QMC data quite well[72] and shows the validity of our DMRG setup and calculation. With growing $J_2$, the Néel order seems to be melted at $J_2 \simeq 0.3$, where the Néel order parameters are smaller than those of the non-magnetic state at $J_2 = 0.5, \Delta = 0$[67,68]. For the larger $J_2$, $m^2_{\rm str}$ becomes finite at $J_2 = 1.2, 1.5$ (see SM for the results of $m^2(0,\pi)$ and $m^2(\pi,0)$[71]), showing the stripe order survived from randomness. The strong average spin correlations at $J_2 = 1.2$ also support the emergent stripe order[71]. Based on the DMRG results, we identify an intermediate non-magnetic phase.

We further explore a possible spin glass phase in this non-magnetic region[45,52]. Spin glass order can be characterized by the spin-freezing parameter $\overline{q}$[73] defined as

$$\overline{q} = \frac{1}{N_s}\sqrt{\sum_{ij}[\langle \mathbf{S}_i \cdot \mathbf{S}_j\rangle^2]}. \tag{3}$$

If spin orientations freeze, $\overline{q}$ would be nonzero in the thermodynamic limit. First of all, we show the size scaling of $\overline{q}$ versus $L_x$ for given $L_y$ ($N_s = L_x \times L_y$ in Eq. (3)) in Fig. 2(c-d). On the $L_y = 4, 6$ systems with large $L_x$, $\overline{q}$ clearly shows the $L_x^{-1/2}$ scaling behavior, agreeing with that in the 1d RS state. We further study the decay behavior of $[\langle \mathbf{S}_i \cdot \mathbf{S}_j\rangle^2]$ as a function of $|i-j|$, which indeed supports this $L_x^{-1/2}$ scaling behavior[71]. We also notice that for any given $L_x$, $\overline{q}$ decreases with growing $L_y$, strongly indicating the absent spin freezing in large-size limit. To confirm this conclusion, we also compute $\overline{q}$ in the middle $L_y \times L_y$ subsystem and analyze $\overline{q}$ versus $1/L_y$ as shown in Fig. 2(e-f). Since the $\overline{q}$ data decrease slightly faster than linear behavior, we linearly extrapolate the results using the two largest-size data to reduce finite-size effect. In the magnetic order phases, $\overline{q}$ goes to finite value as expected. In the non-magnetic region, we can also obtain a very small finite $\overline{q}$ that agrees with the ED conclusion[52] if we use linear scaling for small-size results, as shown by the solid line in Fig. 2(f). However, by fitting the larger-size data, $\overline{q}$ tends to vanish for $L_y \to \infty$, which agrees with the results shown in Fig. 2(c-d). The finite $\overline{q}$ in the ED calculation[52] should be owing to the larger size effect.

*Average and typical spin correlations.* Next, we study the average and typical spin correlations to characterize this disordered phase. We analyze the average spin correlation in two ways. First, we consider the $L_y$-dependence, which has been used in the study of the $J-Q$ model[55]. We calculate the average absolute spin correlations that are defined for the largest-distance sites on the middle $L_y \times L_y$ subsystem, as illustrated in the inset of Fig. 3(a). The log-log plot of the average spin correlation versus $L_y$ shows a power-law decay $C_s(L_y) \propto L_y^{-\alpha}$ with the exponent $\alpha \simeq 2$. This exponent agrees with that found in the RS state of the $J-Q$ model[55]. Secondly we study the average spin correlation decay along the $x$ direction. To reduce finite-size effects, we consider the large systems with $L_y = 8, 10$ and $L_x = 2L_y$. We choose the reference site $\mathbf{S}_0$ on the left side of the middle $L_y \times L_y$ subsystem and study the spin correlation decay $[|\langle \mathbf{S}_0 \cdot \mathbf{S}_r\rangle|]$ from the left to the right side, as shown in Fig. 3(b). The average spin correlations shown here are very close, showing small finite-size effects and the consistent power-law decay $C_s(r) \propto r^{-2}$ (see SM for the smaller-size data and the consistent results for the weaker randomness strength, as well as the preliminary results of the dimer-dimer correlations[71]).

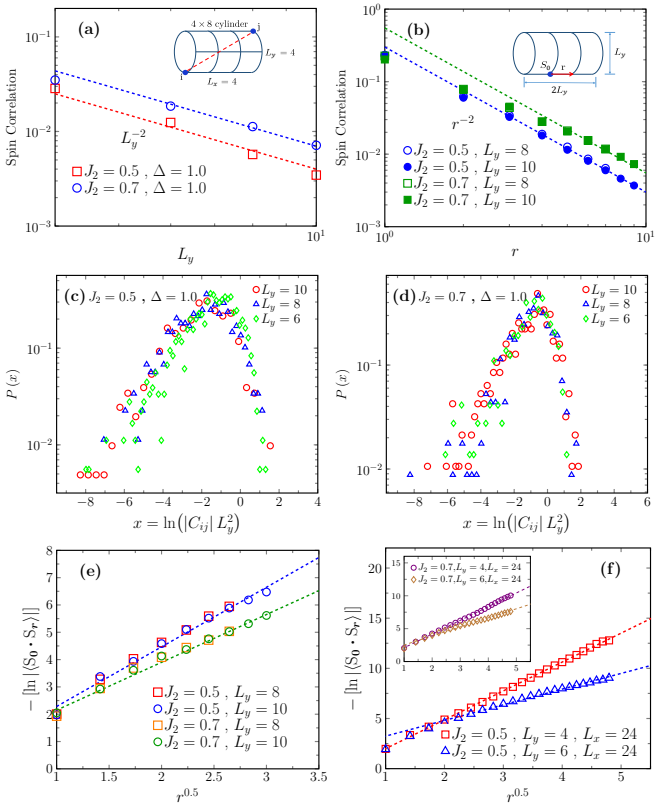



FIG. 3. Size scaling and distribution of spin correlation functions. (a) Log-log plot of the average absolute spin correlation versus $L_y$, which are defined for the largest-distance sites on the middle $L_y \times L_y$ subsystem as shown by the example in the inset. The dashed lines denote the fittings with $C_s(L_y) \sim L_y^{-2}$. (b) Log-log plot of the average absolute spin correlation $[|\langle \mathbf{S}_0 \cdot \mathbf{S}_r\rangle|]$ versus distance $r$ along the axis direction of cylinder. The reference site $\mathbf{S}_0$ is defined on the left side of the middle $L_y \times L_y$ subsystem, and the site $\mathbf{S}_r$ is counted from the left to the right side, as shown by the inset. The dashed lines denote the fittings with $C_s(r) \sim r^{-2}$. (c) and (d) show the data collapse of $P(x)$ versus $x = \ln(|C_{ij}|L_y^2)$ on different system sizes. (e) and (f) show the linear plot of $-[\ln|\langle \mathbf{S}_0 \cdot \mathbf{S}_r\rangle|]$ versus $r^{1/2}$.

We further investigate the probability distribution of the absolute spin correlations defined for the largest-distance sites in the middle $L_y \times L_y$ subsystem, denoted as $|C_{ij}|$. The probability $P(|C_{ij}|)$ versus $\ln|C_{ij}|$ on different sizes becomes broader with growing $L_y$[71], which agrees with the decrease of $C_s(L_y)$ . To eliminate the finite-size effects in the analysis, we define a new scaling variable $x = \ln(|C_{ij}|L_y^2)$ and plot $P(x)$ versus $x$ in Fig. 3(c-d). Any distribution $P(x)$ with data collapse for different $L_y$ must lead to the power-law decay of the average spin correlation

$$C_s(L_y) = \int_0^\infty dx P(x)\frac{e^x}{L_y^2} \propto L_y^{-2}. \tag{4}$$

Thus, the good data collapse in Fig. 3(c-d) further supports

the power-law decay of $C_s(L_y)$ found in Fig. 3(a).

The logarithmically broad distribution of spin correlations may lead to the exponential decay of the typical spin correlation defined as $\exp\left[\ln|\langle \mathbf{S}_0 \cdot \mathbf{S}_r\rangle|\right]$. In the 1d RS state, the exponential typical spin correlation can be equivalently described as $-[\ln|\langle \mathbf{S}_0 \cdot \mathbf{S}_r\rangle|] \propto r^{1/2}$[23]. We show the linear plot of $-[\ln|\langle \mathbf{S}_0 \cdot \mathbf{S}_r\rangle|]$ versus $r^{1/2}$ in Fig. 3(e-f). On both the $L_y = 8, 10, L_x = 2L_y$ systems and the $L_y = 4, 6$ cylinders with large $L_x$, $-[\ln|\langle \mathbf{S}_0 \cdot \mathbf{S}_r\rangle|]$ follows the linear scaling with $r^{1/2}$ quite well. We also analyze $-[\ln|\langle \mathbf{S}_0 \cdot \mathbf{S}_r\rangle|]$ versus $r$ using the log-log manner[71], which shows good power-law dependence and the slope gives the power exponent very close to $1/2$, supporting the results in Fig. 3(e-f). Therefore, our results unveil the characteristic behaviors of spin correlations, which suggest the RS nature of this disordered phase.

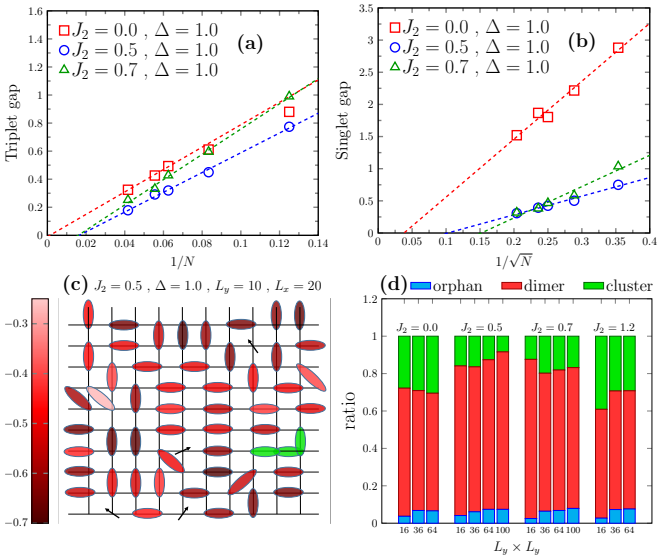



FIG. 4. Finite-size scaling of gaps and distributions of microscopic clusters. (a) and (b) are the gaps obtained from the ED calculation. $N = 8, 12, 16, 18, 24$ is the total site number. The linear fitting curves are guides to the eye. (c) The covering of the isolated dimers (the red ellipse), the resonating-dimer clusters (the connected green ellipses), and the orphan spins (the arrow) on the lattice with a given random sample. The gradation of the red color corresponds to the strength of the bond correlation $\langle \mathbf{S}_i \cdot \mathbf{S}_j\rangle$. (d) The ratios of the different clusters in different quantum phases. We analyze the data from the middle $L_y \times L_y$ subsystem.

*Excitation gaps and microscopic clusters.* The previous ED study found the vanished spin gap in the disordered phase[52]. To further unveil the properties of excitations, we separately compute spin-triplet and singlet gaps by using ED. Compared with the results in the Néel phase, both triplet and singlet gaps in the disordered phase decrease, as shown in Fig. 4(a-b), showing the vanished gaps in the thermodynamic limit[74]. In particular, while the finite-size data of triplet gap slightly decreases, the singlet gap is strongly suppressed.

In the presence of disorder, local clusters may form in microscopic scale. Recent ED study has found three types of clusters in random spin systems, including the isolated dimer, the resonating-dimer cluster, and the orphan spin[53], which should be helpful for understanding low-energy excitations. We extend such analysis in different phases based on the DMRG results. For each sample on the $L_x = 2L_y$ cylinder, we collect all the correlations $\langle \mathbf{S}_i \cdot \mathbf{S}_j\rangle$ in the middle $L_y \times L_y$ subsystem. We define the isolated dimer as the singlet pair with strong correlation, the resonating-dimer cluster as the cluster with more than two strongly-coupled spins, and the orphan spin as the one weakly coupled to other spins (see SM[71] and Ref. 53 for the procedure to obtain the covering of clusters). One example of the covering is shown in Fig. 4(c). For each random sample we compute the ratios for the different types of clusters and then take their sample averages, as shown in Fig. 4(d). In the three quantum phases, the dominant cluster is always the isolated dimer due to strong bond randomness, and the ratio of orphan spin varies slightly. A feature in the disordered state is the less resonating dimers compared with magnetic states. In the RS picture, the triplet excitations are related to breaking dimers. The broad distribution of bond couplings cause a decrease of the triplet excitation gap. For singlet excitations which are related with spin flip in magnetic phases, in the RS state such excitations could be driven by the diffusion of orphan spins[53], which may account for the strongly suppressed singlet gap in Fig. 4(b). Due to the size limit, here we only focus on the features of the small clusters. The collective properties on the larger length scale need future study beyond the present system size.

*Conclusion and discussion.* We have studied the ground states of the spin-$1/2$ square Heisenberg model with random $J_1, J_2$ couplings in the strong disorder regime by using the large-scale DMRG calculation. With growing $J_2$, we find a gapless phase without any magnetic order or spin glass order. We identify the characteristic size-scaling behaviors of spin correlations in this state, including the $L_x^{-1/2}$ scaling of spin-freezing parameter with system length $L_x$, the $r^{-2}$ power-law decay of the average spin correlation, and the exponential decay of the typical spin correlation. Although the RS state of a generic 2d system is not well understood, our results strongly suggest this disordered state as the 2d analog of the 1d RS state. The same scaling behavior of average spin correlation in this frustrated model and the $J-Q$ model also suggests the same fixed point of the states in these different systems. For further study, the dynamic exponent may be explored by the tensor network simulation at finite temperature[75,76] or the analysis of excitation gap distribution (a rough estimation of dynamic exponent from ED gap data is shown in SM[71]).

For $Sr_2CuTe_{1-x}W_xO_6$, spin freezing has been excluded for $x = 0.5$[56], which agrees with our results. For more mixing ratios, the new $\mu$SR measurement has identified a large dynamic exponent supporting the intermediate RS phase in $Sr_2CuTe_{1-x}W_xO_6$[64]. At last, we emphasize that this 2d RS state should be considered as the preliminary understanding of the spin-liquid-like state in $Sr_2CuTe_{1-x}W_xO_6$, since the bond randomness in our study is a simplified picture to describe the random substitution in $Sr_2CuTe_{1-x}W_xO_6$[64]. We leave the more realistic modeling of the material to future study.

*Acknowledgement.* We acknowledge the discussions with Hikaru Kawamura, Victor Quito, Yu-Cheng Lin, and Anders Sandvik. This work was supported by the National Natu-

ral Science Foundation of China grants 11874078, 11834014, grant 11804401, and the Fundamental Research Funds for the Central Universities. The work at CSUN was supported by the U.S. Department of Energy, Office of Basic Energy Sciences under the grant No. DE-FG02-06ER46305 (D.N.S.).

* wuhanq3@mail.sysu.edu.cn
† donna.sheng1@csun.edu
‡ shoushu.gong@buaa.edu.cn

[1] Claudine Lacroix, Philippe Mendels, and Frederic Mila, "Introduction to frustrated magnetism: Materials, experiments, theory," Springer (2013).
[2] Leon Balents, "Spin liquids in frustrated magnets," Nature **464**, 199–208 (2010).
[3] Lucile Savary and Leon Balents, "Quantum spin liquids: a review," Reports on Progress in Physics **80**, 016502 (2016).
[4] M. R. Norman, "Colloquium," Rev. Mod. Phys. **88**, 041002 (2016).
[5] Yi Zhou, Kazushi Kanoda, and Tai-Kai Ng, "Quantum spin liquid states," Rev. Mod. Phys. **89**, 025003 (2017).
[6] X. G. Wen, "Mean-field theory of spin-liquid states with finite energy gap and topological orders," Phys. Rev. B **44**, 2664–2672 (1991).
[7] N. Read and Subir Sachdev, "Large-n expansion for frustrated quantum antiferromagnets," Phys. Rev. Lett. **66**, 1773–1776 (1991).
[8] Xie Chen, Zheng-Cheng Gu, and Xiao-Gang Wen, "Local unitary transformation, long-range quantum entanglement, wave function renormalization, and topological order," Phys. Rev. B **82**, 155138 (2010).
[9] A. Kitaev, "Anyons in an exactly solved model and beyond," Annals of Physics **321**, 2–111 (2006).
[10] B. Fåk, E. Kermarrec, L. Messio, B. Bernu, C. Lhuillier, F. Bert, P. Mendels, B. Koteswararao, F. Bouquet, J. Ollivier, A. D. Hillier, A. Amato, R. H. Colman, and A. S. Wills, "Kapellasite: A kagome quantum spin liquid with competing interactions," Phys. Rev. Lett. **109**, 037208 (2012).
[11] Y. Shimizu, K. Miyagawa, K. Kanoda, M. Maesato, and G. Saito, "Spin liquid state in an organic mott insulator with a triangular lattice," Phys. Rev. Lett. **91**, 107001 (2003).
[12] Satoshi Yamashita, Yasuhiro Nakazawa, Masaharu Oguni, Yugo Oshima, Hiroyuki Nojiri, Yasuhiro Shimizu, Kazuya Miyagawa, and Kazushi Kanoda, "Thermodynamic properties of a spin-1/2 spin-liquid state in a $\kappa$-type organic salt," Nature Physics **4**, 459 (2008).
[13] Y. Li, H. Liao, Z. Zhang, S. Li, F. Jin, L. Ling, L. Zhang, Y. Zou, L. Pi, Z. Yang, J. Wang, Z. Wu, and Q. Zhang, "Gapless quantum spin liquid ground state in the two-dimensional spin-1/2 triangular antiferromagnet ybmggao$_4$," Scientific Reports **5**, 16419 (2015).
[14] Yuesheng Li, Gang Chen, Wei Tong, Li Pi, Juanjuan Liu, Zhaorong Yang, Xiaoqun Wang, and Qingming Zhang, "Rare-earth triangular lattice spin liquid: A single-crystal study of $\mathrm{ybmggao_4}$," Phys. Rev. Lett. **115**, 167203 (2015).
[15] Yao Shen, Yao-Dong Li, Hongliang Wo, Yuesheng Li, Shoudong Shen, Bingying Pan, Qisi Wang, H. C. Walker, P. Steffens, M. Boehm, Yiqing Hao, D. L. Quintero-Castro, L. W. Harriger, M. D. Frontzek, Lijie Hao, Siqin Meng, Qingming Zhang, Gang Chen, and Jun Zhao, "Evidence for a spinon fermi surface in a triangular-lattice quantum-spin-liquid candidate," Nature **540**, 559 (2016).
[16] Joseph A. M. Paddison, Marcus Daum, Zhiling Dun, Georg Ehlers, Yaohua Liu, Matthew B. Stone, Haidong Zhou, and Martin Mourigal, "Continuous excitations of the triangular-lattice quantum spin liquid ybmggao4," Nature Physics **13**, 117 (2016).
[17] Danna E. Freedman, Tianheng H. Han, Andrea Prodi, Peter Muller, Qing-Zhen Huang, Yu-Sheng Chen, Samuel M. Webb, Young S. Lee, Tyrel M. McQueen, and Daniel G. Nocera, "Site specific x-ray anomalous dispersion of the geometrically frustrated kagome magnet, herbertsmithite, zncu3(oh)6cl2," Journal of the American Chemical Society **132**, 16185 (2010).
[18] M. Zhu, D. Do, C. R. Dela Cruz, Z. Dun, H. D. Zhou, S. D. Mahanti, and X. Ke, "Tuning the magnetic exchange via a control of orbital hybridization in $\mathrm{cr_2(te_{1-x}w_x)o_6}$," Phys. Rev. Lett. **113**, 076406 (2014).
[19] Shang-keng Ma, Chandan Dasgupta, and Chin-kun Hu, "Random antiferromagnetic chain," Phys. Rev. Lett. **43**, 1434–1437 (1979).
[20] Chandan Dasgupta and Shang-keng Ma, "Low-temperature properties of the random heisenberg antiferromagnetic chain," Phys. Rev. B **22**, 1305–1319 (1980).
[21] R. N. Bhatt and P. A. Lee, "Scaling studies of highly disordered spin-1/2 antiferromagnetic systems," Phys. Rev. Lett. **48**, 344–347 (1982).
[22] Daniel S. Fisher, "Random transverse field ising spin chains," Phys. Rev. Lett. **69**, 534–537 (1992).
[23] Daniel S. Fisher, "Random antiferromagnetic quantum spin chains," Phys. Rev. B **50**, 3799–3821 (1994).
[24] Daniel S. Fisher, "Critical behavior of random transverse-field ising spin chains," Phys. Rev. B **51**, 6411–6461 (1995).
[25] R. Mélin, Y.-C. Lin, P. Lajkó, H. Rieger, and F. Iglói, "Strongly disordered spin ladders," Phys. Rev. B **65**, 104415 (2002).
[26] Gil Refael, Stefan Kehrein, and Daniel S. Fisher, "Spin reduction transition in spin-$\frac{3}{2}$ random heisenberg chains," Phys. Rev. B **66**, 060402 (2002).
[27] Yu-Rong Shu, Dao-Xin Yao, Chih-Wei Ke, Yu-Cheng Lin, and Anders W. Sandvik, "Properties of the random-singlet phase: From the disordered heisenberg chain to an amorphous valence-bond solid," Phys. Rev. B **94**, 174442 (2016).
[28] L. N. Bulaevskiĭ, A. V. Zvarykina, Yu. S. Karimov, R. B. Lyubovskii, and I. F. Shchegolev, "Magnetic properties of linear conducting chains," Soviet Journal of Experimental and Theoretical Physics **35**, 384 (1972).
[29] Tu N. Nguyen, Patrick A. Lee, and Hans-Conrad zur Loye, "Design of a random quantum spin chain paramagnet: $\mathrm{Sr_3cupt_{0.5}ir_{0.5}o_6}$," Science **271**, 489–491 (1996).
[30] Asad Niazi, E.V. Sampathkumaran, P.L. Paulose, D. Eckert, A. Handstein, and K.-H. Müller, "Sr3cuiro6, a spin-chain compound with random ferromagnetic–antiferromagnetic interactions," Solid State Communications **120**, 11–15 (2001).
[31] Tota Nakamura, "Antiferromagnetic order in an ferromagnetic–antiferromagnetic random alternating quantum spin chain: (ch3)2chnh3cu(clx br1-x)3," Journal of the Physical Society of Japan **72**, 789–792 (2003).
[32] T. Shiroka, F. Casola, V. Glazkov, A. Zheludev, K. Prša, H.-R. Ott, and J. Mesot, "Distribution of nmr relaxations in a random heisenberg chain," Phys. Rev. Lett. **106**, 137202 (2011).
[33] T. Shiroka, F. Eggenschwiler, H.-R. Ott, and J. Mesot, "From order to randomness: Onset and evolution of the random-singlet state in bond-disordered $\mathrm{bacu_2(Si_{1-x}Ge_x)_2o_7}$ spin-chain com-

pounds," Phys. Rev. B **99**, 035116 (2019).
[34] Pavel A. Volkov, Choong-Jae Won, D. I. Gorbunov, Jaewook Kim, Mai Ye, Heung-Sik Kim, J. H. Pixley, Sang-Wook Cheong, and G. Blumberg, "Random singlet state in $ba_5cuir_3o_{12}$ single crystals," Phys. Rev. B **101**, 020406 (2020).
[35] Toshio Ono, Hidekazu Tanaka, Takamitsu Nakagomi, Oleksandr Kolomiyets, Hiroyuki Mitamura, Fumihiro Ishikawa, Tsuneaki Goto, Kenji Nakajima, Akira Oosawa, Yoshihiro Koike, Kazuhisa Kakurai, Jens Klenke, Peter Smeibidle, Michael Meiner, and Hiroko Aruga Katori, "Phase transitions and disorder effects in pure and doped frustrated quantum antiferromagnet cs2cubr4," Journal of the Physical Society of Japan **74**, 135–144 (2005), https://doi.org/10.1143/JPSJS.74S.135.
[36] Kazuya Katayama, Nobuyuki Kurita, and Hidekazu Tanaka, "Quantum phase transition between disordered and ordered states in the spin-$\frac{1}{2}$ kagome lattice antiferromagnet $(Rb_{1-x}Cs_x)_2cu_3snf_{12}$," Phys. Rev. B **91**, 214429 (2015).
[37] T. Furukawa, K. Miyagawa, T. Itou, M. Ito, H. Taniguchi, M. Saito, S. Iguchi, T. Sasaki, and K. Kanoda, "Quantum spin liquid emerging from antiferromagnetic order by introducing disorder," Phys. Rev. Lett. **115**, 077001 (2015).
[38] Hironori Yamaguchi, Masataka Okada, Yohei Kono, Shunichiro Kittaka, Toshiro Sakakibara, Toshiki Okabe, Yoshiki Iwasaki, and Yuko Hosokoshi, "Randomness-induced quantum spin liquid on honeycomb lattice," Scientific Reports **7**, 16144 (2017).
[39] Lucile Savary and Leon Balents, "Disorder-induced quantum spin liquid in spin ice pyrochlores," Phys. Rev. Lett. **118**, 087203 (2017).
[40] Olexei Motrunich, Siun-Chuon Mau, David A. Huse, and Daniel S. Fisher, "Infinite-randomness quantum ising critical fixed points," Phys. Rev. B **61**, 1160–1172 (2000).
[41] István A. Kovács and Ferenc Iglói, "Infinite-disorder scaling of random quantum magnets in three and higher dimensions," Phys. Rev. B **83**, 174207 (2011).
[42] Thomas Vojta, Adam Farquhar, and Jason Mast, "Infinite-randomness critical point in the two-dimensional disordered contact process," Phys. Rev. E **79**, 011111 (2009).
[43] Thomas Vojta, Chetan Kotabage, and José A. Hoyos, "Infinite-randomness quantum critical points induced by dissipation," Phys. Rev. B **79**, 024401 (2009).
[44] J. Oitmaa and O. P. Sushkov, "Two-dimensional randomly frustrated spin- $1/2$ heisenberg model," Phys. Rev. Lett. **87**, 167206 (2001).
[45] Y.-C. Lin, R. Mélin, H. Rieger, and F. Iglói, "Low-energy fixed points of random heisenberg models," Phys. Rev. B **68**, 024424 (2003).
[46] Itamar Kimchi, John P. Sheckelton, Tyrel M. McQueen, and Patrick A. Lee, "Scaling and data collapse from local moments in frustrated disordered quantum spin systems," Nature Communications **9**, 4367 (2018).
[47] Ken Watanabe, Hikaru Kawamura, Hiroki Nakano, and Toru Sakai, "Quantum spin-liquid behavior in the spin-1/2 random heisenberg antiferromagnet on the triangular lattice," Journal of the Physical Society of Japan **83**, 034714 (2014).
[48] Hikaru Kawamura, Ken Watanabe, and Tokuro Shimokawa, "Quantum spin-liquid behavior in the spin-1/2 random-bond heisenberg antiferromagnet on the kagome lattice," Journal of the Physical Society of Japan **83**, 103704 (2014).
[49] Tokuro Shimokawa, Ken Watanabe, and Hikaru Kawamura, "Static and dynamical spin correlations of the $s = \frac{1}{2}$ random-bond antiferromagnetic heisenberg model on the triangular and kagome lattices," Phys. Rev. B **92**, 134407 (2015).
[50] Kazuki Uematsu and Hikaru Kawamura, "Randomness-induced quantum spin liquid behavior in the s = 1/2 random j1-j2 heisenberg antiferromagnet on the honeycomb lattice," Journal of the Physical Society of Japan **86**, 044704 (2017).
[51] Han-Qing Wu, Shou-Shu Gong, and D. N. Sheng, "Randomness-induced spin-liquid-like phase in the spin-$\frac{1}{2}$ $J_1 - J_2$ triangular heisenberg model," Phys. Rev. B **99**, 085141 (2019).
[52] Kazuki Uematsu and Hikaru Kawamura, "Randomness-induced quantum spin liquid behavior in the $s = \frac{1}{2}$ random $J_1-J_2$ heisenberg antiferromagnet on the square lattice," Phys. Rev. B **98**, 134427 (2018).
[53] Hikaru Kawamura and Kazuki Uematsu, "Nature of the randomness-induced quantum spin liquids in two dimensions," Journal of Physics: Condensed Matter **31**, 504003 (2019).
[54] R. R. P. Singh, "Valence bond glass phase in dilute kagome antiferromagnets," Phys. Rev. Lett. **104**, 177203 (2010).
[55] Lu Liu, Hui Shao, Yu-Cheng Lin, Wenan Guo, and Anders W. Sandvik, "Random-singlet phase in disordered two-dimensional quantum magnets," Phys. Rev. X **8**, 041040 (2018).
[56] O. Mustonen, S. Vasala, E. Sadrollahi, K. P. Schmidt, C. Baines, H. C. Walker, I. Terasaki, F. J. Litterst, E. Baggio-Saitovitch, and M. Karppinen, "Spin-liquid-like state in a spin-1/2 square-lattice antiferromagnet perovskite induced by d10–d0 cation mixing," Nature Communications **9**, 1085 (2018).
[57] O. Mustonen, S. Vasala, K. P. Schmidt, E. Sadrollahi, H. C. Walker, I. Terasaki, F. J. Litterst, E. Baggio-Saitovitch, and M. Karppinen, "Tuning the $s = 1/2$ square-lattice antiferromagnet $Sr_2Cu(Te_{1-x}w_x)o_6$ from néel order to quantum disorder to columnar order," Phys. Rev. B **98**, 064411 (2018).
[58] Masari Watanabe, Nobuyuki Kurita, Hidekazu Tanaka, Wataru Ueno, Kazuki Matsui, and Takayuki Goto, "Valence-bond-glass state with a singlet gap in the spin-$\frac{1}{2}$ square-lattice random $J_1-J_2$ heisenberg antiferromagnet $sr_2cute_{1-x}w_xo_6$," Phys. Rev. B **98**, 054422 (2018).
[59] S. Vasala, M. Avdeev, S. Danilkin, O. Chmaissem, and M. Karppinen, "Magnetic structure of sr2cuwo6," Journal of Physics: Condensed Matter **26**, 496001 (2014).
[60] P. Babkevich, Vamshi M. Katukuri, B. Fåk, S. Rols, T. Fennell, D. Pajić, H. Tanaka, T. Pardini, R. R. P. Singh, A. Mitrushchenkov, O. V. Yazyev, and H. M. Rønnow, "Magnetic excitations and electronic interactions in $sr_2cuteo_6$: A spin-$1/2$ square lattice heisenberg antiferromagnet," Phys. Rev. Lett. **117**, 237203 (2016).
[61] H. C. Walker, O. Mustonen, S. Vasala, D. J. Voneshen, M. D. Le, D. T. Adroja, and M. Karppinen, "Spin wave excitations in the tetragonal double perovskite $sr_2cuwo_6$," Phys. Rev. B **94**, 064411 (2016).
[62] Tomoyuki Koga, Nobuyuki Kurita, Maxim Avdeev, Sergey Danilkin, Taku J. Sato, and Hidekazu Tanaka, "Magnetic structure of the $s = \frac{1}{2}$ quasi-two-dimensional square-lattice heisenberg antiferromagnet $sr_2cuteo_6$," Phys. Rev. B **93**, 054426 (2016).
[63] Vamshi M. Katukuri, P. Babkevich, O. Mustonen, H. C. Walker, B. Fåk, S. Vasala, M. Karppinen, H. M. Rønnow, and O. V. Yazyev, "Exchange interactions mediated by nonmagnetic cations in double perovskites," Phys. Rev. Lett. **124**, 077202 (2020).
[64] Wenshan Hong, Lu Liu, Chang Liu, Xiaoyan Ma, Akihiro Koda, Xin Li, Jianming Song, Wenyun Yang, Jinbo Yang, Peng Cheng, Hongxia Zhang, Wei Bao, Xiaobai Ma, Dongfeng Chen, Kai Sun, Wenan Guo, Huiqian Luo, Anders W. Sandvik, and Shiliang Li, "Extreme suppression of antiferromagnetic order and critical scaling in a two-dimensional random quantum magnet," Phys. Rev. Lett. **126**, 037201 (2021).
[65] P. Chandra and B. Doucot, "Possible spin-liquid state at large $s$ for the frustrated square heisenberg lattice," Phys. Rev. B **38**, 9335–9338 (1988).
[66] Subir Sachdev and R. N. Bhatt, "Bond-operator representation of

quantum spins: Mean-field theory of frustrated quantum heisenberg antiferromagnets," Phys. Rev. B **41**, 9323–9329 (1990).

[67] Shou-Shu Gong, Wei Zhu, D. N. Sheng, Olexei I. Motrunich, and Matthew P. A. Fisher, "Plaquette ordered phase and quantum phase diagram in the spin-$\frac{1}{2}$ $J_1-J_2$ square heisenberg model," Phys. Rev. Lett. **113**, 027201 (2014).

[68] Wen-Yuan Liu, Shou-Shu Gong, Yu-Bin Li, Didier Poilblanc, Wei-Qiang Chen, and Zheng-Cheng Gu, "Gapless quantum spin liquid and global phase diagram of the spin-1/2 j1-j2 square antiferromagnetic heisenberg model," Science Bulletin **67**, 1034–1041 (2022).

[69] Steven R. White, "Density matrix formulation for quantum renormalization groups," Phys. Rev. Lett. **69**, 2863–2866 (1992).

[70] I. P. McCulloch and M. Gulácsi, "The non-abelian density matrix renormalization group algorithm," Europhysics Letters **57**, 852–858 (2002).

[71] See Supplemental Material for more details.

[72] Nicolas Laflorencie, Stefan Wessel, Andreas Läuchli, and Heiko Rieger, "Random-exchange quantum heisenberg antiferromagnets on a square lattice," Phys. Rev. B **73**, 060403 (2006).

[73] K. Binder and A. P. Young, "Spin glasses: Experimental facts, theoretical concepts, and open questions," Rev. Mod. Phys. **58**, 801–976 (1986).

[74] Since the Néel and stripe antiferromagnetic phase break SU(2) symmetry spontaneously in the thermodynamic limit, the energy spectrum has the Anderson tower of states on finite-size systems. With growing system size, the tower of states levels scale with $1/N$ to the ground state, and the low-energy magnon excitations scale with $1/\sqrt{N}$, where $N$ is the total number of sites. Therefore, we scale the triplet gap with $1/N$ and singlet gap with $1/\sqrt{N}$.

[75] Bin-Bin Chen, Lei Chen, Ziyu Chen, Wei Li, and Andreas Weichselbaum, "Exponential thermal tensor network approach for quantum lattice models," Phys. Rev. X **8**, 031082 (2018).

[76] Han Li, Yuan Da Liao, Bin-Bin Chen, Xu-Tao Zeng, Xian-Lei Sheng, Yang Qi, Zi Yang Meng, and Wei Li, "Kosterlitz-thouless melting of magnetic order in the triangular quantum ising material tmmggao4," Nature Communications **11**, 1111 (2020).